PERGAMON

Mechatronics 11 (2001) 79–94

MECHATRONICS

Development of two-axis arm motion generator using active impedance

Se-Han Lee, Jae-Bok Song*

Department of Mechanical Engineering, Korea University, 5-Ka Anam-Dong Sungbuk-Ku Seoul, 136-701, South Korea

Received 2 January 1999; accepted 17 December 1999

Abstract

In this research a two-dimensional arm motion generator, composed of two linear motors, was developed. The inertia, damping and/or stiffness characteristics of the motion generator can be changed on the real-time basis by properly regulating the force generated by the linear motors. That is, active impedance is implemented without actual change in the physical structure of the motion generator. Control of the motor force is carried out by regulating the input currents supplied to the linear motors by using a common voltage-driven driver. In the control system, the time delay due to A/D conversion of the current output has an adverse effect on the stability of the system. Furthermore, disturbances caused by characteristics of the motion generator also exist. To cope with these difficulties, a 2-DOF controller combined with LQ-servo and H-infinity controllers was used. The gains of the controller are selected so that disturbance rejection, stability guarantee and tracking performance may be achieved. This motion generator can be used to measure kinesthetic sense associated with the human arm and thus leads to developing the products for which the kinesthetic sense is taken into account.

Keywords: Arm motion generator; Active impedance; 2-DOF controller; H-infinity controller; Linear motor

* Corresponding author. Tel.: +82-2-3290-3363; fax: +82-2-3290-3757.
E-mail address: jbsong@korea.ac.kr (J.-B. Song).

0957-4158/01/$ - see front matter
PII: S0957-4158(00)00010-6

1. Introduction

As lifestyles modernize, products with not only function but also kinesthetic sense along with function draw customers, attention. That is, people consider the sensibility of a product as well as its performance. In recent years, there has been a lot of efforts to apply this to products even though in the early stages of development.

The objective of this research is to develop an arm motion generator necessary for quantification and implementation of kinesthetic sense, which mainly relates to arm movement. In most mechanical systems, motion has a close relationship with mechanical impedance, which consists of inertia, stiffness, and damping. Therefore, the arm motion generator developed in this research work xsis capable of measuring the kinesthetic sense difference as experienced by a person by altering the mechanical impedance and can let the person to experience the desired kinesthetic sense. But varying the impedance physically is very tedious, costly, and time demanding. The arm motion generator controls the force and output of the linear motors so that it may have the same effect of physically changing the impedance. In addition, use of two linear motors makes two-dimensional movement possible.

These kinds of motion generators are used in various flight and vehicle simulators, and vigorous research continues today in this field. However, these motion generators use mainly pneumatic systems to generate an entire body movement, and thus systems get complicated and manufacturing becomes costly. But since the motion generator developed in this research only deals with arm movement, it makes use of an electric motor possible, which makes system composing and controlling simple.

The similar concept of active impedance used in this research has also been studied in robot engineering. In robotics,when a manipulator is in contact with an object,the relation between the force exerted on the object by the manipulator and the motion at the contact point is modeled with impedance such as inertia,damping and stiffness and then the appropriate position/force control is carried out [1,2]. In this research, the concept of active impedance is basically the same as the impedance control in robotics,but has many differences in application purpose and method.

Section 2 of this paper takes a closer look at the hardware structure of the arm motion generator and Section 3 handles the concept of active impedance. Section 4 deals with the 2-DOF control system including the LQ servo and H-infinity controllers. In Section 5, examples of active impedance implementation, using the arm motion generator developed in this research, are given.

2. Structure of arm motion generator

An arm motion generator capable of implementing two-dimensional plane motion (i.e., x and y axes) was made by combining two identical linear motors

perpendicularly as shown in Fig. 1. An operator grasps the lever attached to the moving part of the upper motor and produces an arbitrary 2D motion by moving the lever in the xy plane. The structure of the arm motion generator should be symmetrical for the x and y axes for true 2D motion; however, it is not symmetrical as far as mass is concerned since the fixed part of the upper linear motor is attached to the moving part of the lower one.

Fig. 2 shows the arm motion generator and drive circuit to run linear motors, TMS320 DSP board is used as a controller, and PC is used to collect and analyze experimental data. The linear motor used here has a 3-phase, 4-pole motor part which consists of permanent magnets and drive coils and an encoder used to track position, combined as one structure. A voltage driven brushless DC (BLDC) drive, exclusively for motors, is used to drive the linear motor. That is, it detects position of the linear motor with Hall sensor signals and applies voltage to the corresponding driving coil in pulse width modulation (PWM) xsmode.

The main controller TMS 320 DSP board can be operated at 40 MHz and it carries out algorithms necessary to control the motor. This board has ± 10 V range, 12-bit resolution A/D and D/A converters. The A/D converter measures analog current supplied to the motor and digitizes it then sends it to the DSP, while the D/A converter transforms the output digital signal from the controller to analog voltage to send it to the motor drive. A PC communicates with the controller through the parallel port and takes charge of collecting and analyzing the experimental data.

3. Implementation of active impedance

3.1. Concept of active impedance

Impedance in a mechanical system is defined as a measure of motion response

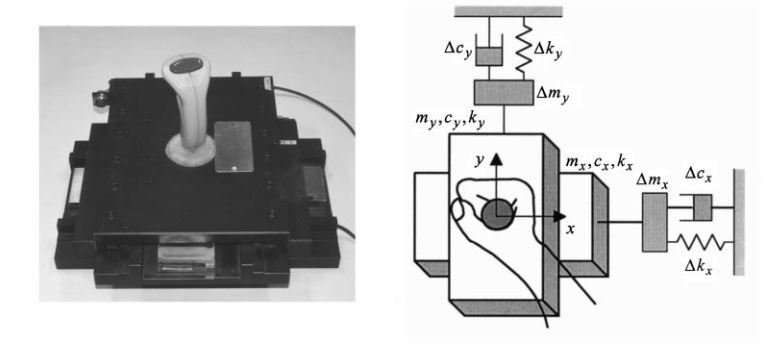

Fig. 1. Configuration of motion generator and concept of active impedance.

to force exerted on the system, and consists of inertia, damping, and stiffness. Active impedance, mentioned in this research, means getting the same effect from physically changing the impedance of the moving part of the linear motor as from only generating the proper force from the motor.

Although the motion generator is capable of 2D movement in the xy plane, only one-dimensional movement is explained here because exactly the same formula can be used for both axes. Let us first consider active inertia. When an operator applies force F to the lever of the deenergized linear motor in which moving part has mass of m, acceleration of $a_0 = F/m$ is experienced. Suppose that the moving part mass is now decreased by Δm (<0) to

$$M = m + \Delta m \tag{1}$$

Then, the operator will experience acceleration of

$$a = \frac{F}{M} = \frac{F}{m + \Delta m} \tag{2}$$

for the same input force F. This change of mass can be achieved by the motor operation without actual change in the physical mass of the moving part. Let us find motor force F_{motor} with which the operator will experience acceleration a (not a_0) even when he exerts the same force F on moving part of mass m.

$$F + F_{\text{motor}} = m \cdot a \tag{3}$$

Combining Eqs. (2) and (3) yields

$$F_{\text{motor}} = -\Delta\, m \cdot a \tag{4}$$

Note that the motor force is in the same direction as the force F given by the operator because $\Delta m < 0$ is assumed in this case. With the aid of the motor force, the acceleration felt by the operator is a ($> a_0$), which is the acceleration obtained

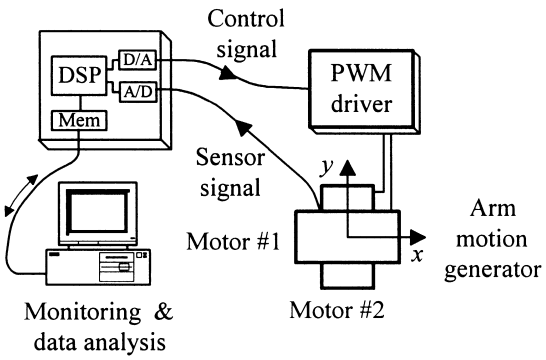

Fig. 2. Schematic experimental setup.

from force F applied to inertia M, even when the operator exerts force F on mass m.

The force generated by a linear motor is $F_{\text{motor}} = K_F i$, where K_F is the force constant of the motor and i is the current supplied to the motor. Thus, supplying the current of

$$i_m = -\Delta m \cdot a / K_F \tag{5}$$

to the motor would generate the effect of active inertia M. Here, the subscript m on the current denotes the current related to mass. If $\Delta m > 0$, on the other hand, the motor force becomes negative (See Eq. (4)) and thus it is in the opposite direction to the force applied by the operator. In this case, the operator will experience acceleration less than $a_o (= F/m)$ for the same input force F.

Active damping C and active stiffness K can be presented in the same manner,

$$C = c + \Delta c, \quad K = k + \Delta k \tag{6}$$

where c and k are the original damping and stiffness of the moving part of the linear motor, and Δc and Δk the added damping and stiffness, respectively. Suitable current values for the motor to obtain these active damping and stiffness are,

$$i_c = -\Delta c \cdot v / K_F, \quad i_k = -\Delta k \cdot x / K_F \tag{7}$$

where v and x are the velocity and the position of the moving part of the linear motor. Since most linear motors have small damping and stiffness characteristics, the active damping and stiffness are usually greater than the original values (i.e., $\Delta c > 0$, $\Delta k > 0$).

3.2. Implementation of active impedance

In some systems, inertia, damping or stiffness characteristics may exist alone, but in most actual mechanical systems they exist in a composite fashion. That is why implementing composite active impedance is required to let us reach closer to actual systems. When an operator applies force to the lever of the arm motion generator, it exerts the same amount of force on his hand in the opposite direction, as noted in Newton's law of action-reaction. This force is called reaction force. Thus, when the operator generates motion by exerting force on the lever connected to the motor, the operator will experience reaction to inertia, damping, and stiffness as follows:

$$F_{\text{total}} = F_{\text{inertia}} + F_{\text{damping}} + F_{\text{stiffness}} = Ma + Cv + Kx \tag{8}$$

When considering a reaction force for the particular instant, it is impossible to discern each component of the reaction force (e.g., no distinction between damping and stiffness forces). But by considering that the reaction due to inertia is proportional to acceleration, damping to velocity, and stiffness to position, one

can measure the form of time-varying reaction which leads to classification of each component of the total reaction.

When the values of active impedance M, C, K which are to be implemented are determined, necessary additional impedance Δm, Δc and Δk can easily be computed by Eqs. (1) and (6). As the operator moves the lever to generate some movement patterns (e.g., rectilinear, circular, oscillatory), position, velocity, and acceleration involved in this pattern are detected. Since the actual force input by the operator on the lever is not known, the values for acceleration a, velocity v, and position x must be obtained by actual measurements rather than by calculation. The position is measured by counting the pulses from the linear optical encoder, whose resolution is 0.5 μm. The velocity is obtained by counting the number of pulses per sampling period and/or measuring the time between successive pulses. The acceleration is obtained by numerically differentiating the velocity value.

Then, the motor generates the following force for implementation of active impedance.

$$F_{\text{motor}} = -(\Delta m \cdot a + \Delta c \cdot v + \Delta k \cdot x) \tag{9}$$

Note that the positive motor force is assumed to be in the same direction as the force by the operator. To generate this force, the current that must be supplied to the linear motor becomes

$$i = i_m + i_c + i_k = \frac{-(\Delta m \cdot a + \Delta c \cdot v + \Delta k \cdot x)}{K_F} \tag{10}$$

To better understand this concept, let us consider the case in which the lever is moving with uniform acceleration a (although it rarely happens in reality, it is easy to visualize). Then, the motor force is given by Eq. (9) and each component

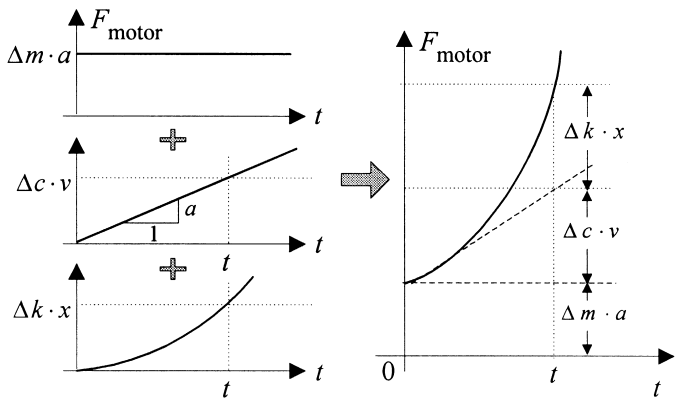

Fig. 3. Motor forces required for active inertia, damping and stiffness during uniformly accelerated motion.

of F_{motor} is shown in Fig. 3, and the current to the motor will be given by

$$i_{\text{total}} = -\frac{\Delta m \cdot a + \Delta c \cdot (at) + \Delta k \cdot \left(\frac{1}{2}at^2\right)}{K_F} \tag{11}$$

Even if an arbitrary motion is made by the operator, the active impedance can be implemented by providing the proper current given by Eq. (10).

By implementing this kind of active impedance (i.e., by varying inertia, damping, and/or stiffness), one can measure the kinesthetic sense most suitable for the operator. The quantitative analysis of such a kinesthetic sense is a different topic, research of which is usually treated in the field of ergonomics. These data can be used to develop products with better kinesthetic sense for the user.

4. Control system

4.1. Control system for arm motion generator

As mentioned before, in order to implement active impedance, control of the force generated by the linear motor is needed. This force is proportional to the current supplied to the motor, and thus force control is performed by current control. Since motor drivers are usually voltage-driven, the current is not directly controlled, but controlled indirectly by controlling the voltage. That is, to supply the necessary current, the voltage of the linear motor must be controlled by the controller on the basis of the difference between the targeted value and the actual value of the current. The relation between the input voltage u and the current i flowing through the motor is commonly known as

$$u - K_E v = L\frac{\mathrm{d}i}{\mathrm{d}t} + Ri \tag{12}$$

where L and R denote the inductance ($\approx$10 mH) and resistance ($\approx$8 Ω) of the linear motor winding, respectively, v the motor velocity, and K_E the back emf constant ($\approx$19 V/(m/s)). The back emf $K_E v$ is generated proportional to the velocity of the motor, and is applied in the opposite direction to the supplied voltage to the motor. Since the position, velocity and acceleration of the arm motion generator depend mostly upon the force arbitrarily applied by the operator, the term $K_E v$ on the left-hand side of Eq. (12) varies arbitrarily. Therefore, this will be treated as disturbance in the control system and then the plant $G(s)$ can be described by

$$G(s) = \frac{I(s)}{U(s)} = \frac{1}{Ls + R} \tag{13}$$

The linear motor drive in Fig. 2 provides the current required for force control

based on the current command. Since the current output is measured by the A/D converter and fed back to the control system, a time delay of at least one sampling period T_s occurs. The electric time constant τ_e of the motor is about 1250 μs, while the sampling period of the control system is set to $T_s = 400$ μs. Since it is generally preferable that the sampling period be less than 1/10 of the plant time constant, the sampling period must decrease to improve stability of the control system. However, there are some difficulties in reducing the sampling period. First, the bandwidth of the motor drive built in this linear motor system is about 2.5 kHz and a faster sampling rate than this bandwidth does not improve the performance. Second, an excessively small sampling period may deteriorate the accuracy of velocity measurement since it is likely that less than a whole pulse appears during one sampling period, especially for low velocity operation. In addition, an excessively small sampling period may cause the acceleration value to fluctuate since it is numerically obtained by dividing the velocity difference of successive samples by the sampling period. For all these reasons as stated above, it is preferable to set a rather large sampling period, which may cause the stability problem as explained below.

Let us investigate the effect of the time delay associated with the sampling period on the control system. Root locus analysis for the discretized electric part of the linear motor is shown in Fig. 4 and it indicates that the proportional gain is limited to about 9.5 for the closed-loop system to be stable. It is noted that infinite gain is allowed in the first-order analog plant as described by Eq. (13). Consider the situation in which the lever is suddenly moved to a certain distance. In this case, a large current must flow in the beginning portion of the movement to implement active impedance. Fig. 5 shows the two experimental results of the current responses with the PI controller. The response (a) with the P gain greater than the critical value 9.5 generates unstable behavior, while the response (b) with the P gain lower than the critical value cannot achieve fast tracking though stable. Therefore, this time delay problem should be properly treated in order to get both stable and good performance. In this research, an H-infinity control scheme is adopted to cope with this problem.

A 2-DOF control system [3,4] has been employed,which includes an LQ-servo

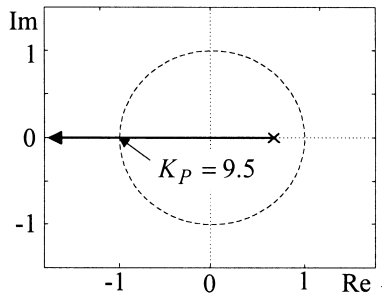

Fig. 4. Root locus of discretized electric part.

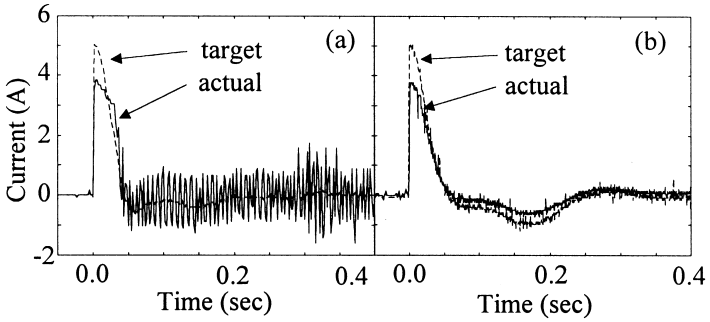

Fig. 5. Current responses with PID controller; (a) high P gain and (b) low P gain.

for feedforward compensation and an H-infinity controller for series compensation as shown in Fig. 6. In this figure, the time delay due to the sampling period is represented by the multiplicative modeling error Δ_m. The LQ-servo controller produces the control input u_m based on the difference of the target current r and the output of the internal plant (Eq. (13)) y_m. Because of the modeling error and neglect of the back emf, $K_E v$, the actual output y and the internal plant output y_m yield some error, which will be treated by the H-infinity controller. The total control input u is computed as the sum of the outputs of the LQ-servo and the H-infinity controllers.

4.2. H-infinity control formulation

As explained before, the time delay related to the sampling period T_s is treated as the multiplicative modeling error Δ_m in Fig. 6. It is well known that robust stability is guaranteed if provided that the multiplicative modeling error Δ_m satisfies the following condition:

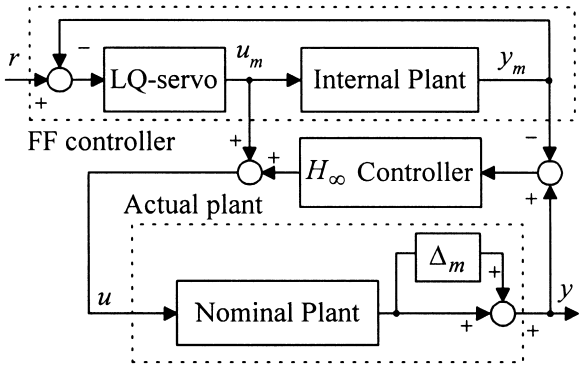

Fig. 6. Block diagram of 2-DOF current controller composed of LQ-servo and H-infinity controllers.

$$|\Delta_m(j\omega)| = |e^{-j\omega T_s} - 1| < |T(j\omega)|^{-1} \quad \text{for all } \omega \tag{14}$$

where $T(s)$ is the nominal cosensitivity function (i.e., closed-loop transfer function). Fig. 7 shows the Bode plot of this multiplicative modeling error. Based on this condition, the cosensitivity weighing function $W_T(s)$ can be selected as an envelope for the multiplicative modeling error [5]

$$W_T(s) = \frac{2.2T_s s}{T_s s + 1} \tag{15}$$

Another weighing function to be considered is a sensitivity weighing function as a performance factor. Since the operator of a motion generator is a human, the activating frequency may be within 20 Hz. Thus, the frequency region here is limited to 50 Hz, which is large enough to cover various patterns of arm motion. The sensitivity weighing function has cutoff frequency of 50 Hz and includes a pure integral part to eliminate a steady-state error caused by constant disturbance.

$$W_S(s) = \frac{50 \times 2\pi}{s(s + 50 \times 2\pi)} \tag{16}$$

The weighing functions $W_T(s)$ and $W_S(s)$ are used for the mixed sensitivity H-infinity control problem shown in Fig. 8. In this figure, w denotes the output y_m of the internal plant and e the error $y_m - y$. The fictitious outputs z_1 and z_2 represent $W_S e$ and $W_T y$, respectively. Then, the generalized plant $P(s)$ can be represented by

$$\begin{Bmatrix} z_1 \\ z_2 \\ e \end{Bmatrix} = \begin{bmatrix} W_S(s) & -W_S(s)G(s) \\ 0 & W_T(s)G(s) \\ I & -G(s) \end{bmatrix} \begin{Bmatrix} w \\ u \end{Bmatrix} = P(s) \begin{Bmatrix} w \\ u \end{Bmatrix} \tag{17}$$

Thus the H-infinity problem becomes

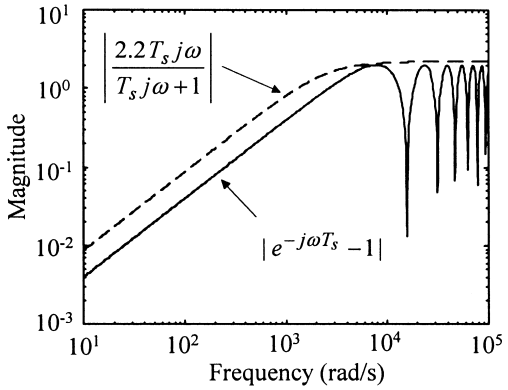

Fig. 7. Bode plots of $\Delta_m(s)$ and $W_T(s)$.

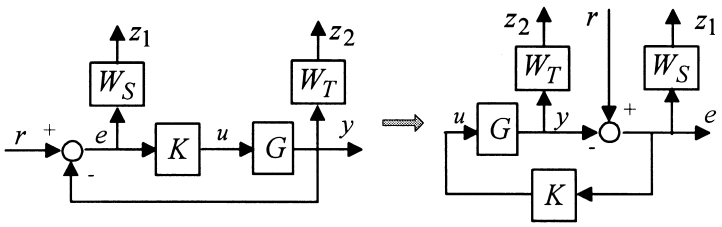

Fig. 8. Mixed sensitivity H-infinity problem with weighing functions.

$$\left\| \begin{matrix} (1/\gamma) \cdot W_S(s)S(s) \\ W_T(s)T(s) \end{matrix} \right\|_\infty < 1 \tag{18}$$

where $S(s)$ is the sensitivity function and γ is a positive real number. At $\gamma \approx 0.14$, the controller $K(s)$ corresponding to Eq. (18) can be obtained [6–8]. The sensitivity and cosensitivity functions and their inverse weighing functions with controller $K(s)$ are shown in Fig. 9. With this plot, it is assured that the condition (18) is satisfied.

4.3. LQ-servo formulation

The LQ-servo is used to control the internal plant. Though finding the proper gains of the LQ-servo problem usually needs trial and error procedure, there is merit in obtaining control gain to consider the control input constraint [9]. In this LQ-servo problem, the following performance index is minimized:

$$J = \int_0^\infty \left(\|y - r\|_Q^2 + \|\dot{u}\|_R^2 \right) \mathrm{d}t \tag{19}$$

Then, the control signal is obtained by

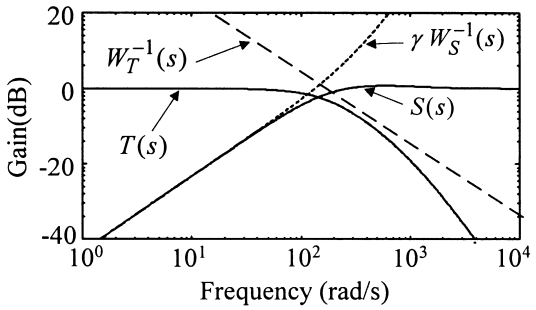

Fig. 9. Sensitivity, cosensitivity functions and their inverse weighing functions.

$$u(t) = -K_1 x(t) + K_2 \int_0^t (y(\tau) - r)\, d\tau \tag{20}$$

assuming that the initial condition $x(0) = 0$. It is noted in Eq. (20) that the second term represents the integral part to eliminate the steady-state error. Fig. 10 shows the block diagram for this LQ-servo scheme. Here, the control input weighing matrix R was chosen so as not to exceed maximum motor drive output.

5. Performance of arm motion generator

5.1. Performance of current controller

Fig. 11 shows the experimental results for the current response with the 2-DOF controller composed of the LQ-servo and H-infinity controllers. The tracking performance is much better than that of the PI controller as shown in Fig. 5. In addition, the stability problem noticed in Fig. 5(a) is of no concern.

Fig. 12 shows the experimental results for the current response when active stiffness is implemented and the operator moves the lever in an oscillatory fashion. Again the 2-DOF controller shown in (a) provides much better performance than the PI controller shown in (b). That is, the actual current can track the oscillatory reference input both accurately and quickly. Similar results were obtained for the cases of active damping and inertia, though omitted here.

5.2. One-dimensional motion generation

In this section, some test results of one-dimensional motion with the lower linear motor fixed are presented. Fig. 13 shows the linear motor having moving part of mass $m = 5.8$ kg, damping coefficient of $c \approx 20$ N s/m, and stiffness of $k \approx 0$. The active stiffness is set to $K = 300$ N/m by setting an additional stiffness of $\Delta k = 300$ N/m. Then, the position of the moving part of the motor is measured each time when the lever is released at the initial position of about 8 cm. As shown in the Fig. 13, the amplitude decreases gradually because the linear motor originally has damping of its own. Therefore, implementation of active impedance on the system enabled the motion generator to vibrate as if it was a spring mechanism.

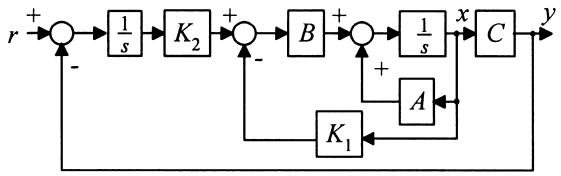

Fig. 10. Block diagram of LQ-servo controller.

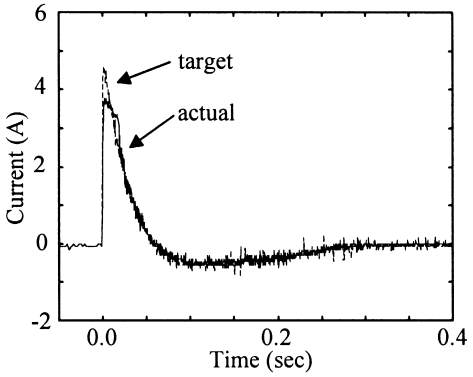

Fig. 11. Current response with 2-DOF controller.

Fig. 14 shows the linear motor having the same specifications as the above one. But this time, not only the active stiffness as in Fig. 13, but also the additional damping of $\Delta c = 60$ N s/m is added. Then, the lever was released at the initial position of about 8 cm. As expected, the vibration fades away more rapidly than before due to additional damping.

5.3. Two-dimensional motion generation

As mentioned before, the structure of the arm motion generator is not symmetrical as far as mass is concerned since the fixed part of the upper linear motor is attached to the moving part of the lower one. Therefore, even if the operator manipulates the lever to draw a circle, it is likely that the trajectory of

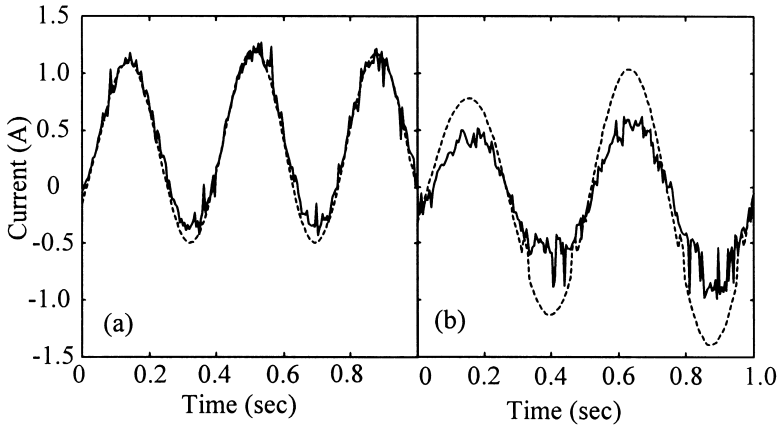

Fig. 12. Current responses of arm motion generator with active stiffness implemented: (a) 2-DOF controller, and (b) PI controller.

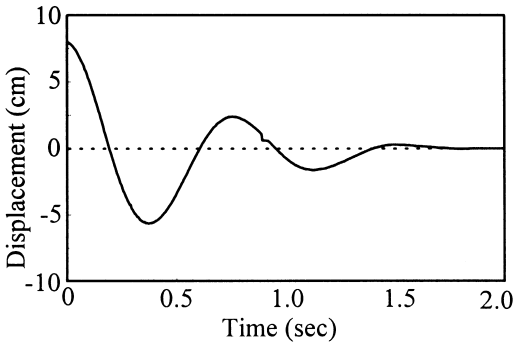

Fig. 13. Displacement response of the motion generator subject to initial displacement with active stiffness implemented.

the lever will become an ellipse due to the unsymmetrical mass distribution. For a true 2D motion generator, it is important to have symmetrical mass distribution. In order to solve this problem, active inertia is implemented when 2D motion is desired.

Since it is not easy for the operator to move the lever in a circular fashion with uniform force for experimental purposes, a simple apparatus was devised for the test as shown in Fig. 15. The lever is replaced by a very flexible rod, which is rotated by a rotary motor moving at a low speed through a speed reducer. The trajectory A in Fig. 16 shows the case in which active inertia is not implemented, where the trajectory of the lever point Q is an ellipse in which the y-axis is the major axis, although the motor-driven end point P of the flexible rod rotates in a circle. This effect is attributed to the uneven mass distribution, in which the mass (about 5.8 kg) along the y-axis is much lighter than that (about 19.7 kg) along the x-axis. However, as the amount of the active inertia along the y-axis increases, the trajectory of the point Q shown in Fig. 16 becomes more circular as expected.

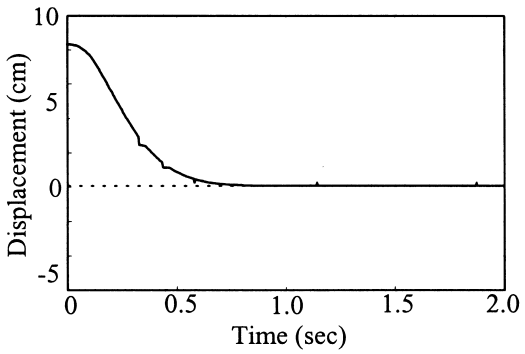

Fig. 14. Displacement response of the motion generator subject to initial displacement with active stiffness and damping implemented.

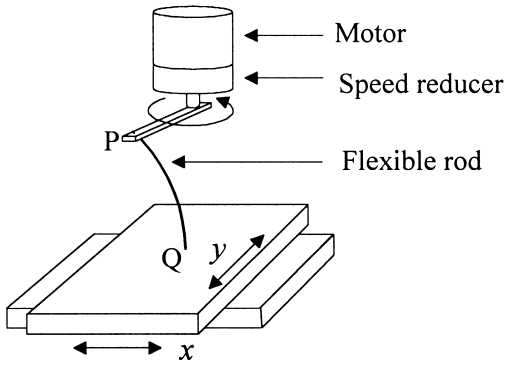

Fig. 15. Test apparatus for active mass implementation.

Like the cases dealt above, the arm motion generator developed in this research and the concept of active impedance can be used to acquire combinations of various active inertia, damping, and/or stiffness. Since these changes in impedance are not obtained from physical structural changes, real-time changes are possible, enabling measurement of diverse kinesthetic senses. For example, while moving the lever, the damping and stiffness can be changed to desired patterns. And at the same time, the kinesthetic sense experienced by the operator can be evaluated.

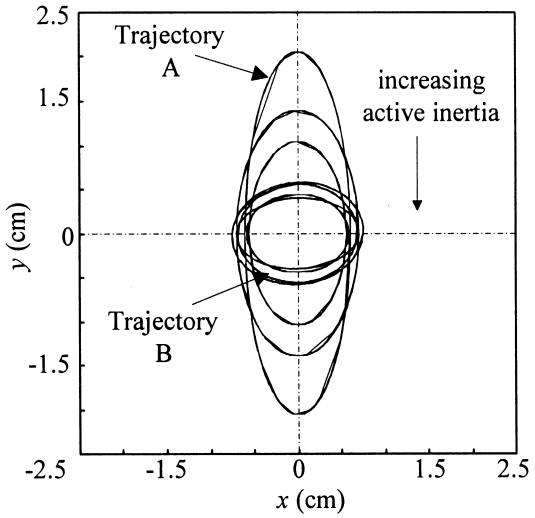

Fig. 16. Change in trajectory of the lever as the amount of active mass increases (trajectory A is without active mass implemented).

6. Conclusions

In this research, an arm motion generator capable of two-dimensional movement was built by perpendicularly connecting two linear motors. By controlling the forces generated by these motors, active impedance is implemented, which has the same effect as physically changing the mass, damping, and/or stiffness of the arm motion generator. Numerous kinesthetic senses relating to arm movement can be evaluated due to the ability to change the impedance, such as mass, damping, and stiffness, on a real-time basis.

In this research, a 2-DOF controller composed of LQ-servo and H-infinity controllers was employed to cope with some inherent problems with current control of the linear motor. The time delay problem related to the limitation on the sampling period was treated as a multiplicative modeling error and an H-infinity controller was used to cope with it. The control system used in this research shows reasonable performance on both stability and tracking compared to the PI controller which has some gain limits due to a low sampling rate.

The arm motion generator built in this research is currently used to evaluate numerous kinesthetic senses related to arm movements. However, the motion is limited to two dimensions and mass is unevenly distributed though overcome by active inertia. The next version of the arm motion generator is now under development, but the idea of active impedance and its control system will be pretty much the same as the one introduced in this article.

References

[1] Spong MW, Vidyasagar M. Robot dynamics and control. New York: Wiley, 1989.
[2] Lewis FL, Abdallah CT, Dawson DM. Control of Robot manipulator. New York: Macmillan, 1993.
[3] Hirata M, Liu K, Mita T, Yamaguchi T. Head positioning control of a hard disk drive using H_∞ theory. In: Proc. 31st Conf. Decision and Control, 1992. p. 2460–1.
[4] Masaki S, Shu Y, Jun S, Kouki M. The basic characteristic of two-degree-of-freedom PID controller using a simple design method for linear servo motor drives. In: Proceedings of Advanced Motion Control, 1997. p. 59–64.
[5] John CD, Francis BA, Tannenbaum AR. Feedback Control theory. New York: Macmillan, 1992.
[6] Kemin ZH, Doyle JC, Glover K. Robust and optimal control. NJ: Prentice-Hall, 1996.
[7] John CD, Keith G, Pramod PK, Bruce AF. State-space solution to standard H_2 and H_∞ control problems. IEEE Transactions on Automatic Control 1989;34(8):831–47.
[8] Bahram S, Hassel M. Control system design using MATLAB. NJ: Prentice-Hall, 1993.
[9] Burl JB. Linear optimal control: H_2 and H_∞ Methods. Reading, MA, USA: Addison-Wesley, 1999.